

Quantum Simulated Annealing

R. D. Somma,^{1,*} S. Boixo,^{2,3} and H. Barnum²

¹*Perimeter Institute for Theoretical Physics, Waterloo, ON N2L 2Y5, Canada*

²*Los Alamos National Laboratory, Los Alamos, NM 87545, USA*

³*Department of Physics and Astronomy, University of New Mexico, Albuquerque, NM 87131, USA*

(Dated: November 26, 2024)

We develop a quantum algorithm to solve combinatorial optimization problems through quantum simulation of a classical annealing process. Our algorithm combines techniques from quantum walks, quantum phase estimation, and quantum Zeno effect. It can be viewed as a quantum analogue of the discrete-time Markov chain Monte Carlo implementation of classical simulated annealing. Our implementation requires order $1/\sqrt{\delta}$ operations to find an optimal solution with bounded error probability, where δ is the minimum spectral gap of the stochastic matrix used in the classical simulation. The quantum algorithm outperforms the classical one, which requires order $1/\delta$ operations.

PACS numbers: 03.67.Ac, 87.10.Rt, 87.55.de

I. INTRODUCTION

Combinatorial optimization problems (COPs) such as the traveling salesman problem are important in almost every branch of science, from computer science to statistical physics and computational biology [1]. A COP consists of a family of *instances* of the problem; each instance is an optimization problem, to minimize (or maximize) some objective function over a finite set \mathcal{S} of d elements, called the space of *states*. This space may have additional structure (e.g., it may be a graph), allowing the definition of a notion of locality; and the set of objective functions may have special properties depending on the particular COP. In general multiple local minima may be present. Finding a solution by exhaustive search is hard in general, due to the large size of the search space. Therefore, more efficient optimization approaches are desirable. Efficiency is typically quantified in terms of how the resources needed to find the optimum scale with the *instance size*, which is typically polynomial in $\log d$.

Simulated Annealing (SA) is a possible generic strategy for solving a COP [2]. The idea of SA is to imitate the process undergone by a metal that is heated to a high temperature and then cooled slowly enough for thermal excitations to prevent it from getting stuck in local minima, so that it ends up in one of its lowest-energy states. In SA, the objective function plays the role of energy, so the lowest energy state is the optimum. This process can be simulated using different techniques; we focus on discrete Markov chain Monte-Carlo (MCMC). These methods are often used to numerically obtain properties of, for example, classical physical lattice systems in equilibrium [3]. The general idea of MCMC is to stochastically generate a sequence of states via a process that converges to a target probability distribution. This is the Boltzmann distribution at the low final temperature in the case of SA. The efficiency of the method relies on the fact that, in general, only a small proportion of states contribute significantly to the determination of properties in equilibrium. Therefore, if a good

state-generating rule is chosen, the MCMC algorithm can explore the most relevant states only, outperforming exhaustive search.

One way to estimate the implementation complexity of SA using MCMC is to count the number of times that the state-generating rule must be executed (i.e., the number of generated states) in order that the desired distribution is reached within an acceptable error. This complexity, denoted by \mathcal{N}_{SA} , is of order $\mathcal{O}(\log(d/\epsilon^2)/\delta)$ (see Sec. II). Here, δ is the minimum spectral gap of the stochastic matrices used to generate states for the COP via MCMC [4], while ϵ is the error probability, that is, the probability that the final state sampled via this process is not a solution (not in the set \mathcal{S}_0 of optimal states). Ideally, \mathcal{N}_{SA} is insignificant compared to the size of the state space. This is the situation, for example, when computing physical properties of the Ising spin model using the Metropolis rule [3]. In this example \mathcal{N}_{SA} is known to be of order $\mathcal{O}(N^2)$ for a system of N spins, while the state space dimension is $d = 2^N$. Nevertheless, \mathcal{N}_{SA} can increase rapidly with N if the interaction strengths are made random [5], making the problem intractable in general. In this case, this is due to the gap δ becoming exponentially small in N (instance size). Therefore, finding new methods with better scaling in δ , yielding speedups over SA, is of great importance.

Quantum mechanics provides new resources with which to attack these optimization problems [6, 7, 8]. Quantum computers (QCs) can theoretically solve some problems, including integer number factorization and search problems, more efficiently than today's conventional computers [9]. Still, whether a QC can solve all COPs more efficiently than its classical counterpart is an open question. In this paper we show that QCs can also be used to speed up the simulation of classical annealing processes. That is, we present a new quantum algorithm that can be seen as the quantum analogue of SA using MCMC, but for which the number of times that the state-generating rule is called (\mathcal{N}_{QSA}) is greatly reduced to $\mathcal{O}(\log^3(d/\epsilon^2)/(\sqrt{\delta}\epsilon^2))$, to achieve error bounded by ϵ , in a single run. This speed-up is most significant for hard instances where $\delta \ll 1$. Our quantum simulated annealing algorithm (QSA) is constructed using ideas and techniques from quantum walks [10, 11] and quantum phase estima-

*Electronic address: somma@lanl.gov

tion [12, 13]. The QSA also exploits the so-called quantum Zeno effect [14, 15], in which after $Q = \mathcal{O}(1/\Delta t)$ measurements of a quantum system at short time-intervals Δt the state is collapsed onto the ground state with total probability $1 - \mathcal{O}(\Delta t)$.

This paper is organized as follows. First, in Sec. II, we describe the implementation of SA using discrete-time MCMC, and in Appendix A we derive a rate at which the temperature of a classical system can be lowered to assure convergence to the set of ground states. To do this we adapt the results obtained for the continuous-time case in Ref. [4]. The rate that we obtain is similar to the one in Ref. [16] for those cases where δ decreases exponentially with the problem size (cf. Ref. [7]). In Sec. III we describe a quantization of a reversible Markov chain in terms of quantum walks. Our quantization is a similarity-transformed version of the one used in Refs. [10, 17] to speed up search problems. It constructs, from the transition matrix of the Markov chain, a unitary operator acting on a set of quantum states corresponding to the classical ones. In Sec. IV we describe our QSA and obtain the corresponding implementation complexity, exhibiting a quantum speed-up with respect to classical SA. Since our QSA makes calls to the phase estimation algorithm, we describe phase estimation in Appendix B. Finally, we present the conclusions in Sec V.

II. SIMULATED ANNEALING AND MONTE-CARLO TECHNIQUES FOR MARKOV PROCESSES

We consider the simulation of a classical annealing process via MCMC, and give annealing rates such that the final sampled state is almost certain to be in the set \mathbb{S}_0 of optimal solutions to a COP. To do this, we first need a formulation of the COP in terms of an equivalent problem in which \mathbb{S}_0 consists of the states that minimize some real-valued cost function E on the state space. Usually, E is regarded as the energy function of a classical system \mathcal{S} , so the optimal solutions to the COP are represented by the ground states of \mathcal{S} . For concreteness, we sometimes think of \mathcal{S} as defined on a lattice with N vertices, having a finite state space $\{\sigma\}$ of size $d = \mathcal{O}(\exp(N))$.

A ground state can be reached by annealing slowly enough, starting with \mathcal{S} at sufficiently high temperature. The MCMC simulation of this process, described in terms of the *inverse temperature* $\beta \equiv 1/T$, begins by sampling a state $\sigma^{(0)}$ from the uniform distribution. The annealing process is determined by a choice of an *annealing schedule*, i.e. a finite increasing sequence $\beta_1 < \beta_2 < \dots < \beta_P$, and by a sequence of *transition rules* $\{M(\beta_k)\}$. Each $M(\beta_k)$ is a stochastic matrix whose elements $m_{\sigma\sigma'}(\beta_k)$ are transition probabilities from σ to σ' . $M(\beta_k)$ is chosen to have the Boltzmann distribution at β_k as its unique equilibrium distribution.

At each step k , a new state $\sigma^{(k)}$ is stochastically generated from $\sigma^{(k-1)}$ according to the transition probabilities $M(\beta_k)$. The annealing schedule is chosen to give an acceptable upper bound ϵ on the probability of error (of not ending up in \mathbb{S}_0). For simplicity, we consider an annealing schedule such that $\Delta\beta = \beta_k - \beta_{k-1} \ll 1$ is constant, and thus $\beta_f \equiv P\Delta\beta$. In

general the annealing schedule may strongly depend on β_k . In our case the overall implementation complexity of the algorithm with constant $\Delta\beta$ is of the same order as for a general annealing schedule, so the analysis below is valid for both situations.

We choose $\Delta\beta = \mathcal{O}(\delta/E_M)$, where δ is the minimum spectral gap of the matrices $M(\beta_k)$ at inverse temperature $\beta_k = k\Delta\beta$, and $E_M := \max_{\sigma} |E[\sigma]|$. In Appendix A we show that for $\beta_f = \mathcal{O}(\gamma^{-1} \log(d/\epsilon^2))$, the probability of not ending in a solution is no greater than ϵ [see Eq. (A19)]. γ is the spectral gap of E . The implementation complexity of SA is then given by $P = \beta_f/\Delta\beta$. We obtain

$$\mathcal{N}_{SA} = \mathcal{O}(\beta_f E_M / \delta) = \mathcal{O}\left(\frac{E_M \log(d/\epsilon^2)}{\gamma \delta}\right) \quad (1)$$

for a success probability greater than $1 - \epsilon$. The dependence of \mathcal{N}_{SA} on δ^{-1} is characteristic of Markov processes and, although Eq. (1) only gives an upper bound on the resources required for the implementation of SA, such a dependence on the spectral gap may be unavoidable [18].

Remarkably, a similar algorithm implemented on a *quantum* computer has a reduced implementation complexity for those hard instances where $\delta \ll 1$. This is described in the following sections.

III. QUANTUM WALKS AND ERGODIC MARKOV CHAINS

Discrete-time quantum walks were introduced as the quantum analogues of classical random walks [19, 20]. Here, we focus on those bipartite quantum walks defined in Refs. [10, 17] for the purpose of obtaining quantum speed-ups in search problems. Such quantum walks, which we describe below, can also be derived from Ref. [11].

To define the bipartite quantum walk, we first associate each classical state σ of \mathcal{S} with a quantum state $|\sigma\rangle$ of an orthonormal basis of a d -dimensional Hilbert space \mathcal{H} . We then consider a tensor product Hilbert space $\mathcal{H}_A \otimes \mathcal{H}_B$ of two copies of \mathcal{H} . As in SA, we assume a given stochastic matrix $M(\beta)$ describing the Markov process in \mathcal{S} , with $M(\beta)$ satisfying the detailed balance condition: $\pi^\sigma m_{\sigma\sigma'} = \pi^{\sigma'} m_{\sigma'\sigma}$, with $\pi^\sigma = e^{-\beta E[\sigma]} / \mathcal{Z}$ the components of the equilibrium distribution ($\mathcal{Z} = \sum_{\sigma} e^{-\beta E[\sigma]}$ is the partition function). In the following we omit the dependence on β unless necessary. We define isometries X and Y that map states of \mathcal{H} to states of $\mathcal{H}_A \otimes \mathcal{H}_B$ as

$$X|\sigma\rangle = |\sigma\rangle \sum_{\sigma'} \sqrt{m_{\sigma\sigma'}} |\sigma'\rangle, \quad (2)$$

$$Y|\sigma'\rangle = \sum_{\sigma} \sqrt{m_{\sigma'\sigma}} |\sigma\rangle |\sigma'\rangle. \quad (3)$$

The symmetric operator $H = X^\dagger Y$, acting on \mathcal{H} , has elements $h_{\sigma\sigma'} = \sqrt{m_{\sigma\sigma'} m_{\sigma'\sigma}}$ [10]. Because of detailed balance, we can write $H \equiv e^{\beta H_c/2} M e^{-\beta H_c/2}$, with H_c the diagonal operator $H_c|\sigma\rangle = E[\sigma]|\sigma\rangle$. Therefore, the eigenvalues

$\lambda_0 = 1 > \lambda_1 \geq \dots \geq \lambda_{d-1} \geq 0$ of H are those of M . If $|\phi_j\rangle$ denotes the eigenstate of H with eigenvalue λ_j , we have for $j = 0$ [7]

$$|\phi_0\rangle \equiv \sum_{\sigma} \sqrt{\pi^{\sigma}} |\sigma\rangle \equiv \frac{e^{-\beta H_c/2}}{\sqrt{\mathcal{Z}}} \sum_{\sigma} |\sigma\rangle. \quad (4)$$

The isometries X and Y define unitary operators U_X and U_Y , acting on $\mathcal{H}_A \otimes \mathcal{H}_B$, via

$$U_X |\sigma \circ\rangle \equiv X |\sigma\rangle, \quad (5)$$

$$U_Y |\circ \sigma\rangle \equiv Y |\sigma\rangle, \quad (6)$$

with $|\circ\rangle$ a selected state in \mathcal{H} . The action of U_X and U_Y in the remaining subspace is irrelevant. We now define R_1 to be the reflection operator through the subspace spanned by $\{|\sigma \circ\rangle\}$ and R_2 the reflection operator through the subspace spanned by $\{U_X^{\dagger} U_Y |\circ \sigma\rangle\}$. Thus,

$$R_1 \equiv 2\Pi_1 - \mathbb{1} \otimes \mathbb{1}, \quad (7)$$

$$R_2 \equiv 2\Pi_2 - \mathbb{1} \otimes \mathbb{1}, \quad (8)$$

where Π_1 and Π_2 are the projectors

$$\Pi_1 \equiv \mathbb{1} \otimes |\circ\rangle\langle\circ|, \quad (9)$$

$$\Pi_2 \equiv U_X^{\dagger} U_Y (|\circ\rangle\langle\circ| \otimes \mathbb{1}) U_Y^{\dagger} U_X. \quad (10)$$

The unitary operation (rotation) $W(M) \equiv R_2 R_1$ defines the bipartite quantum walk based on the Markov chain M . This walk is related to the one used in Refs. [10, 17] by a unitary, but β -dependent, similarity transformation; using the transformed version is necessary for our QSA to work.

The spectrum of $W(M)$ can be directly related to the spectrum of M [10]. Defining the phases $\varphi_j \equiv \arccos \lambda_j$, so that

$$H |\phi_j\rangle = \cos \varphi_j |\phi_j\rangle = X^{\dagger} Y |\phi_j\rangle, \quad (11)$$

we have $\varphi_0 = 0$. When $\varphi_1 \ll 1$, the spectral gap of M (or H) is $1 - \lambda_1 \approx (\varphi_1)^2/2$. From Eqs. (5) and (6),

$$\Pi_1 U_X^{\dagger} U_Y |\circ \phi_j\rangle = \cos \varphi_j |\phi_j \circ\rangle \quad (12)$$

$$\Pi_2 |\phi_j \circ\rangle = \cos \varphi_j U_X^{\dagger} U_Y |\circ \phi_j\rangle, \quad (13)$$

so the action of $W(M)$ in the (at most) two-dimensional subspace spanned by $\{|\phi_j \circ\rangle, U_X^{\dagger} U_Y |\circ \phi_j\rangle\}$ is an overall $4\varphi_j$ rotation along an axis perpendicular to that subspace [21]. Thus the eigenphases of $W(M)$ are $\pm 2\varphi_j$, and its eigenvectors for $j \neq 0$ are:

$$|\psi_{\pm j}\rangle = \frac{\pm i}{\sqrt{2} \sin \varphi_j} \left(e^{\mp i \varphi_j} |\phi_j \circ\rangle - U_X^{\dagger} U_Y |\circ \phi_j\rangle \right). \quad (14)$$

When $j = 0$, we have

$$|\psi_0\rangle \equiv |\phi_0 \circ\rangle, \quad (15)$$

so a quantum algorithm that prepares the *quantum Gibbs* state $|\psi_0\rangle$ allows us to sample from the desired (equilibrium) distribution by measuring \mathcal{H}_A in the basis $\{|\sigma\rangle\}$. All the other

eigenphases of $W(M)$ that were not described are either 0 or π .

The (quantum) implementation complexity of U_X and U_Y is proportional to the (classical) implementation complexity of a single step of the MCMC method described in Sec. II, because U_X , U_X^{\dagger} , U_Y , and U_Y^{\dagger} may be implemented using a *reversible* version of the classical algorithm that computes a matrix element of M . It follows that the implementation complexity of $W(M)$ is proportional to the classical complexity of implementing four steps in the MCMC method.

The operations $W(M)$ will be used below to implement the QSA. An important property that follows from our definition of $W(M)$ is that the overlap between the quantum Gibbs state $|\psi_0(\beta)\rangle$ and any other eigenstate in the 0-eigenphase subspace, at any β' , is zero. To show this note that $|\phi_j\rangle$ is a complete basis for \mathcal{H} , and $|\phi_j \circ\rangle = \frac{1}{\sqrt{2}}[|\psi_{+j}\rangle + |\psi_{-j}\rangle]$ ($j \neq 0$). Thus,

$$|\psi_0(\beta)\rangle = \sum_{j=0}^{d-1} c_j |\phi_j(\beta') \circ\rangle \quad (16)$$

$$= c_0 |\psi_0(\beta')\rangle + \sum_{j=1}^{d-1} \frac{c_j}{\sqrt{2}} [|\psi_{+j}(\beta')\rangle + |\psi_{-j}(\beta')\rangle].$$

Our algorithm uses this property to keep the state $|\psi_0(\beta)\rangle$ separated from the remaining degenerate subspace.

IV. QUANTUM SIMULATED ANNEALING ALGORITHM

The QSA that we propose is basically a sequence of phase estimation algorithms (PEAs) projecting onto the quantum Gibbs state that is associated with the equilibrium state of \mathcal{S} for different temperatures. The implementation complexity of SA is dominated by the gap of the stochastic matrix, which constrains the annealing schedule. For the QSA algorithm, the total implementation complexity is dominated by the implementation complexity of each PEA, given by the eigenphase gap of the quantum walk. Because the latter is (quadratically) larger than the former, the QSA algorithm results in a (quadratic) quantum speed-up of SA.

We consider a sequence of inverse temperatures $\{\beta_k = k\Delta\beta\}$, with $k = 1, \dots, Q$, and $\beta_f = \beta_Q = Q\Delta\beta$. The choice of $\Delta\beta$ differs from the one used for SA. To understand the QSA, we begin by performing a Taylor series expansion of $|\phi_0(\beta_{k-1})\rangle$ [Eq. (4)] in β_k . We obtain,

$$|\phi_0(\beta_{k-1})\rangle = \left(1 - \frac{\Delta\beta}{2} (\langle E \rangle_{\beta_k} - H_c) \right) |\phi_0(\beta_k)\rangle + \mathcal{O}(\nu^2), \quad (17)$$

where $\langle E \rangle_{\beta_k} = \sum_{\sigma} E[\sigma] e^{-(\beta_k) E[\sigma]} / \mathcal{Z}(\beta_k) \equiv \langle \phi_0(\beta_k) | H_c | \phi_0(\beta_k) \rangle$ is the expectation value of the energy (cost function), and $\nu = \Delta\beta E_M$. The (squared) overlap for two adjacent values of β is

$$|\langle \phi_0(\beta_k) | \phi_0(\beta_{k-1}) \rangle|^2 = 1 - \mathcal{O}(\nu^2). \quad (18)$$

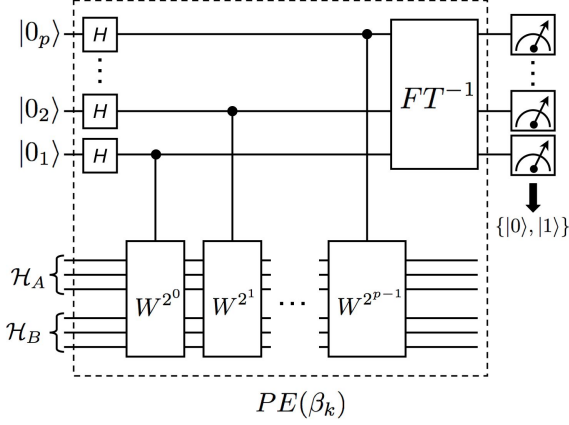


FIG. 1: Phase estimation algorithm (subroutine) for the quantum simulated annealing algorithm. The first register of p qubits is used to encode the eigenphases of $W(M(\beta_k))$. The second register denotes the bipartite system $\mathcal{H}_A \otimes \mathcal{H}_B$. The algorithm takes as input, in the second register, a quantum state sufficiently close to $|\psi_0(\beta_{k-1})\rangle$. A sequence of controlled $W(M(\beta_{k+1}))$ operations is performed and the inverse of the quantum Fourier transform is then applied; the composition of all these unitary operations is denoted $PE(\beta_k)$. Finally, the first register is measured. When the result of the measurement is such that the first register is projected onto $|0\rangle = |0_1 \dots 0_p\rangle$, the PEA outputs a state close to $|\psi_0(\beta_k)\rangle$ in the second register.

It follows that the probability of successful preparation of $|\phi_0(\beta_f)\rangle$, after $Q = \mathcal{O}(1/\nu)$ projective measurements, can be bounded below by $1 - \mathcal{O}(\nu)$. This is called the quantum Zeno effect [14, 15]. Our QSA algorithm performs such projections by calling the PEA at β_1, \dots, β_f . This technique was used in Ref. [22] to obtain the quadratic quantum speed-up for Grover's unstructured search problem.

The PEA at the k th step is depicted in Fig. 1. The p ancillary qubits composing the first register are used to encode the eigenphases of $W(M(\beta_k))$ as binary fractions. In particular, $2\varphi_0 = 0 = |0_1 \dots 0_p\rangle_2$. The integer p is chosen to satisfy $2^p = \mathcal{O}(1/(\nu\sqrt{\delta}))$. This choice allows us to bound the error due to the impossibility of representing the phases $2\varphi_j$ with p bits (see Appendix B and Ref. [12]). The PEA gets as input a state close to $|\psi_0(\beta_{k-1})\rangle$. It starts with a sequence of unitary gates that includes $2^p - 1$ actions of the operation $cW(M) = cR_2 cR_1 = U_X^\dagger U_Y cP_{\circ_A} U_Y^\dagger U_X cP_{\circ_B}$, controlled on the states $|1_i\rangle$ of the first register ($i = 1, \dots, p$). Here, cP_{\circ_A} and cP_{\circ_B} are the controlled selective sign change operations on the states $|\circ\rangle$ of \mathcal{H}_A and \mathcal{H}_B , respectively. It continues with an inverse quantum Fourier transform, and finally the first register is measured in the computational basis. For the given input state, the PEA outputs a state close to $|\psi_0(\beta_k)\rangle$ with probability close to one. Since each use of $cW(M(\beta_k))$ has complexity proportional to that of four steps of the classical MCMC method, the overall implementation complexity of the PEA is $\mathcal{N}_{PEA} = \mathcal{O}(1/(\nu\sqrt{\delta}))$.

The QSA is depicted in Fig. 2. It is composed of Q calls to the PEA, with a final measurement of \mathcal{H}_A in the $|\sigma\rangle$ -basis. In

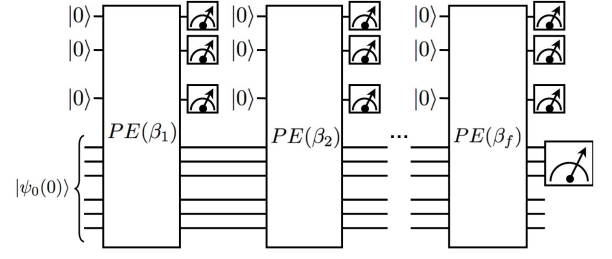


FIG. 2: Quantum simulated annealing algorithm. The algorithm is a sequence of Q calls to the PEA at β_1, \dots, β_f . After the last call, the state of $\mathcal{H}_A \otimes \mathcal{H}_B$ is close to $|\psi_0(\beta_f)\rangle \equiv |\phi_0(\beta_f)\circ\rangle$, with probability close to one. A measurement on \mathcal{H}_A returns a state σ in the ground state space of S with probability greater than $1 - \epsilon$.

Appendix B we show that, after the measurement, the probability of finding \mathcal{H}_A in the excited space can be bounded as

$$\mathcal{P}(\sigma \notin \mathbb{S}_0) \leq de^{-\beta_f \gamma} + \tau' Q \nu^2, \quad (19)$$

for some constant $\tau' = \mathcal{O}(1)$. We seek to make the above error of order ϵ . Choosing $\beta_f = \gamma^{-1} \log(2d/\epsilon^2)$, as in SA, makes the first term on the right hand side of Eq. (19) of order $\mathcal{O}(\epsilon^2)$. Thus we need $\tau' Q \nu^2 = \mathcal{O}(\epsilon)$. The condition $Q \Delta\beta = \beta_f$ implies $\Delta\beta = \mathcal{O}(\epsilon/(\beta_f E_M^2))$ and $Q = \mathcal{O}((\beta_f E_M)^2/\epsilon)$. Finally, because $\mathcal{N}_{QSA} = \mathcal{O}(Q \mathcal{N}_{PEA})$, we obtain

$$\mathcal{N}_{QSA} = \mathcal{O}\left(\frac{(\beta_f E_M)^3}{\epsilon^2 \sqrt{\delta}}\right) = \mathcal{O}\left(\left(\frac{E_M}{\gamma}\right)^3 \frac{\log^3(2d/\epsilon^2)}{\epsilon^2 \sqrt{\delta}}\right). \quad (20)$$

The above scaling with $1/\epsilon^2$ is for a single run of the QSA. Typically, repetition of the QSA makes the error exponentially low in the amount of resources used, so the dependence of \mathcal{N}_{QSA} on ϵ can be made logarithmic. The cubic scaling with the parameter E_M/γ is also worse than classical SA's linear scaling, but this is relatively unimportant as in most applications this parameter will be bounded by a constant or a polynomial in instance size.

Note that, since only the state of \mathcal{H}_A is important for our purposes, the QSA can be implemented without measuring the ancillary qubits used in each PEA. In this case, the operations FT^{-1} can be avoided [22]. This is because the quantum Zeno effect relies on the *decoherence* introduced by the interaction with the ancillae, not the measurement itself.

V. CONCLUSIONS

We have presented a quantum algorithm to simulate classical annealing processes by quantization of the simulated annealing algorithm implemented with MCMC methods. Such a quantization has been done by using techniques borrowed from quantum walks and quantum phase estimation. Our algorithm also exploits the quantum Zeno effect. We have shown that, if ϵ denotes an upper bound to the probability of

not finding an optimal solution to a COP, the QSA requires resources $\mathcal{N}_{QSA} = \mathcal{O}\left(\frac{\log^3(2d/\epsilon^2)}{\epsilon^2\sqrt{\delta}}\right)$, with δ the spectral gap. Thus QSA outperforms SA in those problems where $\delta \ll 1$, such as finding a ground state of a spin glass. SA requires $\mathcal{N}_{SA} = \mathcal{O}(\log(d/\epsilon^2)/\delta)$ to assure the same error probability. Even if SA could be implemented more efficiently, the scaling of \mathcal{N}_{SA} with δ^{-1} may be unavoidable [18]. Since initializing with a state close to $|\phi_0(\beta_f)\rangle$ is not required by the QSA, our result has implications in the mixing time problem studied in Ref. [23].

We expect that similar quantum speed-ups hold for the simulation of more general classical annealing processes. Moreover, our algorithm can easily be extended to simulate continuous-time annealing. Also, by choosing $\beta_f = 1/T$, with $T > 0$, the QSA can be used to speed up the calculation of finite-temperature thermodynamic properties of classical systems on a lattice.

Finally, our QSA is one possible quantum algorithm to simulate an annealing process. One may wonder if other quantum algorithms, based on quantum adiabatic evolutions, can still provide similar quantum speed-ups. The adiabatic theorem of quantum mechanics yields similar convergence rates. A simple, but not rigorous, proof is given by considering the adiabatic condition (cf. [24]):

$$\partial_t \beta(t) \left| \frac{\langle \psi_{\pm j}(\beta) | \partial_\beta \psi_0(\beta) \rangle}{2\varphi_j} \right| \leq \partial_t \beta(t) \frac{E_M}{2\varphi_1} \leq \epsilon, \quad (21)$$

with $j \neq 0$. Other 0-eigenphase states have not been considered as they do not overlap with $|\psi_0(\beta)\rangle$ at first order [Eq. (16)]. The overall implementation complexity of the adiabatic evolution (i.e., total evolution time) determined by Eq. (21) is $\mathcal{O}(1/(\epsilon\sqrt{\delta}))$. Details will be given elsewhere.

Acknowledgments

We thank Stephen Jordan for discussions and for pointing out Ref. [22]. This research was supported by Perimeter Institute for Theoretical Physics. Research at Perimeter Institute is supported by the Government of Canada through Industry Canada and by the Province of Ontario through the Ministry of Research and Innovation. This work was also carried out partially under the auspices of the NNSA of the US DOE at LANL under Contract No. DE-AC52-06NA25396 and by NSF Grant No. PHY-0653596.

APPENDIX A: CONVERGENCE OF CLASSICAL SIMULATED ANNEALING

We now obtain an annealing schedule that assures convergence to the desired state when SA is implemented using discrete MCMC methods. The following analysis is based on Ref. [4], where similar rates have been obtained in the continuous-time case. Assume that we start with a state sampled from some probability vector $\vec{\mu}(0) = \frac{1}{d}(1, \dots, 1)$ (i.e.,

the uniform distribution). After P steps, this state evolves to

$$\vec{\mu}(\beta_f) = (\mu^1(\beta_f), \dots, \mu^d(\beta_f)) = \left(\prod_{k=1}^P M(\beta_k) \right) \vec{\mu}(0), \quad (A1)$$

with $\beta_k = k\Delta\beta$. Because M is stochastic, normalization is preserved: $\sum_{\sigma=1}^d \mu^\sigma(\beta_f) = 1$. Let $\vec{\pi}(\beta_f) = (\pi^1(\beta_f), \dots, \pi^d(\beta_f))$ be the desired (Boltzmann) equilibrium distribution after the annealing process. That is, $M(\beta_f)\vec{\pi}(\beta_f) \equiv \vec{\pi}(\beta_f)$, and also $\sum_{\sigma=1}^d \pi^\sigma(\beta_f) = 1$. From the Cauchy-Schwarz inequality we obtain, for the probability of error,

$$\begin{aligned} \mathcal{P}(\sigma^{(P)} \notin \mathbb{S}_0) &= \sum_{\sigma \notin \mathbb{S}_0} \mu^\sigma(\beta_f) \\ &\leq \sqrt{\left[\sum_{\sigma=1}^d \frac{(\mu^\sigma(\beta_f))^2}{\pi^\sigma(\beta_f)} \right] \left[\sum_{\sigma \notin \mathbb{S}_0} \pi^\sigma(\beta_f) \right]}. \end{aligned} \quad (A2)$$

Considering the worst case, in which all non-ground states have energy $E[\mathbb{S}_0] + \gamma$ gives:

$$\sqrt{\sum_{\sigma \notin \mathbb{S}_0} \pi^\sigma(\beta_f)} \leq \sqrt{d} e^{-\beta_f \gamma/2}, \quad (A3)$$

where $\gamma = \min_{\sigma \notin \mathbb{S}_0} |E[\sigma] - E[\mathbb{S}_0]|$ is the spectral gap of E and d is the dimension of the state space \mathcal{S} . Equation (A3) was obtained considering the worst case scenario in which the space of states having energy $E[\mathbb{S}_0] + \gamma$ is highly degenerate. Thus

$$\mathcal{P}(\sigma^{(P)} \notin \mathbb{S}_0) \leq \sqrt{d} e^{-\beta_f \gamma/2} \|\vec{h}(\beta_f)\|_2, \quad (A4)$$

where $\|\vec{h}(\beta_f)\|_2$ denotes the 2-norm of

$$\vec{h}(\beta_f) \equiv \left(\frac{\mu^1(\beta_f)}{\sqrt{\pi^1(\beta_f)}}, \dots, \frac{\mu^d(\beta_f)}{\sqrt{\pi^d(\beta_f)}} \right). \quad (A5)$$

To bound $\|\vec{h}(\beta_f)\|_2$, we define, as in Sec. III, the symmetric matrix $H(\beta_k) \equiv e^{\beta_k H_c/2} M(\beta_k) e^{-\beta_k H_c/2}$, with H_c the diagonal matrix having $E[1], \dots, E[d]$ as elements. We denote by $\lambda_1(\beta_k) = 1 > \lambda_2(\beta_k) \geq \dots \geq \lambda_d(\beta_k) \geq 0$ the eigenvalues of $M(\beta_k)$ and $H(\beta_k)$. The eigenvector of $H(\beta_k)$ with largest eigenvalue is [7]

$$\begin{aligned} \sqrt{\vec{\pi}(\beta_k)} &= \left(\sqrt{\pi^1(\beta_k)}, \dots, \sqrt{\pi^d(\beta_k)} \right) \\ &\equiv \frac{1}{\sqrt{\mathcal{Z}}} \left(e^{-\beta_k E[1]/2}, \dots, e^{-\beta_k E[d]/2} \right), \end{aligned} \quad (A6)$$

where $\mathcal{Z} = \sum_{\sigma=1}^d e^{-\beta_k E[\sigma]}$ is the partition function. Denote now as $\delta = \min_k \{1 - \lambda_2(\beta_k)\}$ the minimum spectral gap of the matrices $H(\beta_k)$ (or $M(\beta_k)$). We will show that, when $\delta \ll 1$, an annealing rate $\Delta\beta$ satisfying

$$\Delta\beta E_M \leq \tau\delta, \quad (A7)$$

implies $\|\vec{h}(\beta_f)\|_2 \leq \sqrt{2}$ [25]. Here, $E_M = \max_\sigma |E[\sigma]|$ and τ is a $\mathcal{O}(1)$ constant.

We start by writing

$$\begin{aligned}\Delta\vec{\mu}(\beta_k) &\equiv \vec{\mu}(\beta_{k+1}) - \vec{\mu}(\beta_k) \\ &= (M(\beta_{k+1}) - \mathbb{I})\vec{\mu}(\beta_k),\end{aligned}\quad (\text{A8})$$

where $\vec{\mu}(\beta_k) = \prod_{k'=1}^k M(\beta_{k'})\vec{\mu}(0)$. Also, from the Taylor series expansion of $\vec{\pi}(\beta_k)$ and using Eq. (A7), we obtain

$$\begin{aligned}\sqrt{\vec{\pi}(\beta_{k+1})} - \sqrt{\vec{\pi}(\beta_k)} &= \\ &= \frac{1}{2}\Delta\beta(\langle E \rangle_{\beta_k} - H_c)\sqrt{\vec{\pi}(\beta_k)} + \mathcal{O}(\delta^2),\end{aligned}\quad (\text{A9})$$

where $\langle E \rangle_{\beta_k} = \sum_{\sigma=1}^d E[\sigma]e^{-\beta_k E[\sigma]}/\mathcal{Z}$ is the expectation value of E at β_k . Combining Eqs. (A8) and (A9), and defining $\vec{h}(\beta_k) = \left(\frac{\mu^1(\beta_k)}{\sqrt{\pi^1(\beta_k)}}, \dots, \frac{\mu^d(\beta_k)}{\sqrt{\pi^d(\beta_k)}}\right)$, we have

$$\begin{aligned}\Delta\vec{h}(\beta_k) &\equiv \vec{h}(\beta_{k+1}) - \vec{h}(\beta_k) \\ &= (H(\beta_{k+1}) - \mathbb{I})\vec{h}(\beta_k)(1 + \mathcal{O}(\delta)) \\ &\quad - \left(\frac{1}{2}\Delta\beta(\langle E \rangle_{\beta_k} - H_c)\right)\vec{h}(\beta_k) + \mathcal{O}(\delta^2).\end{aligned}\quad (\text{A10})$$

Therefore, if $\langle \cdot, \cdot \rangle$ refers to the standard inner product,

$$\begin{aligned}\langle \vec{h}(\beta_k), \Delta\vec{h}(\beta_k) \rangle &= \\ &= \langle \vec{h}(\beta_k), (H(\beta_{k+1}) - \mathbb{I})\vec{h}(\beta_k) \rangle (1 + \mathcal{O}(\delta)) \\ &\quad - \frac{1}{2}\Delta\beta \langle \vec{h}(\beta_k), (\langle E \rangle_{\beta_k} - H_c)\vec{h}(\beta_k) \rangle + \mathcal{O}(\delta^2).\end{aligned}\quad (\text{A11})$$

The first term in Eq. (A11) can be bounded by expanding $\vec{h}(\beta_k)$ as a sum of the eigenvectors of $H(\beta_{k+1})$, denoted as $\{\vec{e}_j(\beta_{k+1})\}$, with $\vec{e}_1(\beta_{k+1}) \equiv \sqrt{\vec{\pi}(\beta_{k+1})}$ [see Eq. (A6)]. Then,

$$\begin{aligned}\langle \vec{h}(\beta_k), (H(\beta_{k+1}) - \mathbb{I})\vec{h}(\beta_k) \rangle (1 + \mathcal{O}(\delta)) \\ \leq -\delta \left(\|\vec{h}(\beta_k)\|_2^2 - 1 \right) + \mathcal{O}(\delta^2).\end{aligned}\quad (\text{A12})$$

This results in

$$\begin{aligned}\langle \vec{h}(\beta_k), \Delta\vec{h}(\beta_k) \rangle \\ \leq \left(-\delta + \frac{1}{2}\Delta\beta E_M \right) \|\vec{h}(\beta_k)\|_2^2 + \delta + \mathcal{O}(\delta^2),\end{aligned}\quad (\text{A13})$$

where we considered that $\langle \vec{h}(\beta_k), H_c \vec{h}(\beta_k) \rangle \leq E_M \|\vec{h}(\beta_k)\|_2^2$ and, with no loss of generality, $\langle E \rangle_{\beta_k} \geq 0$. Therefore, the increment on $\|\vec{h}(\beta_k)\|_2$ can be bounded as

$$\begin{aligned}\Delta\|\vec{h}(\beta_k)\|_2^2 &\equiv \|\vec{h}(\beta_{k+1})\|_2^2 - \|\vec{h}(\beta_k)\|_2^2 \\ &= 2\langle \vec{h}(\beta_k), \Delta\vec{h}(\beta_k) \rangle + \|\Delta\vec{h}(\beta_k)\|_2^2\end{aligned}\quad (\text{A14})$$

$$\begin{aligned}&\leq (-2\delta + \Delta\beta E_M) \|\vec{h}(\beta_k)\|_2^2 \\ &\quad + 2\delta + \mathcal{O}(\delta^2).\end{aligned}\quad (\text{A15})$$

Since $\|\vec{h}(\beta_k)\|_2^2 \geq 1$ we have, for a proper choice of $\tau = \mathcal{O}(1)$ in Eq. (A7),

$$\Delta\|\vec{h}(\beta_k)\|_2^2 \leq -\delta\|\vec{h}(\beta_k)\|_2^2 + 2\delta. \quad (\text{A16})$$

Equivalently,

$$\|\vec{h}(\beta_{k+1})\|_2^2 \leq (1 - \delta)\|\vec{h}(\beta_k)\|_2^2 + 2\delta. \quad (\text{A17})$$

Furthermore, the condition $\vec{\pi}(0) \equiv \vec{\mu}(0)$ yields to $\|\vec{h}(0)\|_2 = 1$. Iterating Eq. (A17) for $k' = 0, \dots, k$, we obtain

$$\|\vec{h}(\beta_k)\|_2^2 \leq 2 - (1 - \delta)^k \leq 2. \quad (\text{A18})$$

Finally, using Eq. (A4), we obtain the desired bound on the probability of error, given by

$$\mathcal{P}(\sigma^{(P)} \notin \mathbb{S}_0) \leq \sqrt{2d} e^{-\beta_f \gamma/2}. \quad (\text{A19})$$

APPENDIX B: IMPLEMENTATION COMPLEXITY OF THE QUANTUM SIMULATED ANNEALING ALGORITHM

We first show how the PEA works for the eigenphases $\pm 2\varphi_j$ of $W(M)$, with $\varphi_0 = 0 < \varphi_1 \leq \dots \leq \varphi_{d-1} \leq \pi/2$. We write

$$2\varphi_j = 2\pi([a_1^j \dots a_p^j]_2 + \zeta_j) \equiv 2\pi\left(\sum_{i=1}^p a_i^j/2^i + \zeta_j\right), \quad (\text{B1})$$

with $|\zeta_j| \leq 1/2^{p+1}$ and $2\pi[a_1^j \dots a_p^j]_2$ the best p -bit approximation to $2\varphi_j$. The PEA (Fig. 1) begins by applying a set of Hadamard gates to the p qubits in the first register, initialized in the state $|0\rangle = |0_1 \dots 0_p\rangle$. These qubits are used to encode the eigenphases as binary fractions at the end of the PEA. The PEA then applies a set of operations $W^{2^{i-1}}(M)$, with $i = 1, \dots, p$, controlled on the states $|1_i\rangle$ of the first register. Consider the case where the initial state of $\mathcal{H}_A \otimes \mathcal{H}_B$ is one of the eigenstates $|\psi_{\pm j}\rangle$ of $W(M)$ [Eqs. (14) and (15)]. The evolved joint state is

$$\begin{aligned}&\frac{1}{\sqrt{2^p}}(|0_1\rangle + e^{\pm i2^0(2\varphi_j)}|1_1\rangle) \dots \\ &\dots (|0_p\rangle + e^{\pm i2^{p-1}(2\varphi_j)}|1_p\rangle)|\psi_{\pm j}\rangle.\end{aligned}\quad (\text{B2})$$

The next step is to apply the inverse of the quantum Fourier transform, denoted by FT^{-1} in Fig. 1, to the first register. Its action is given by

$$FT^{-1}|m\rangle = \frac{1}{\sqrt{2^p}} \sum_{m'=0}^{2^p-1} e^{-i2\pi mm'/2^p} |m'\rangle, \quad (\text{B3})$$

where $m, m' \in [0, \dots, 2^p - 1]$ are natural numbers whose binary representation denotes the states of qubits $1, \dots, p$. The evolved (joint) state is now

$$|\eta\rangle = \frac{1}{2^p} \sum_{m=0, m'=0}^{2^p-1} e^{-i2\pi mm'/2^p} e^{\pm im'(2\varphi_j)} |m\rangle |\psi_{\pm j}\rangle. \quad (\text{B4})$$

The final step of the PEA is to perform a projective measurement of the first register in the (computational) $\{|0_i\rangle, |1_i\rangle\}$ -basis ($i = 1, \dots, p$). The probability of projecting the first register onto some state $|m\rangle$ is determined by $|o_{\pm j, m}|^2$, with

$$\begin{aligned} o_{\pm j, m} &\equiv \langle m | \psi_j | \eta \rangle \\ &= \frac{1}{2^p} \sum_{m'=0}^{2^p-1} e^{-i2\pi m m' / 2^p} e^{i m' (2\varphi_j)} \\ &= \frac{1}{2^p} \frac{1 - e^{i[2^p(2\varphi_j) - 2\pi m]}}{1 - e^{i(2\varphi_j - 2\pi m/2^p)}}. \end{aligned} \quad (\text{B5})$$

In particular, $o_{0, m} = \delta_{0, m}$ and, since $|1 - e^{ix}| \geq 2|x|/\pi$, we have $|o_{\pm j, m=0}| \leq \pi/(2^p(2\varphi_j))$. The error is due to the fact that, in general, $2\varphi_j$ does not admit an exact representation using p bits.

Clearly, the implementation complexity \mathcal{N}_{PEA} of the PEA is of order $\mathcal{O}(2^p)$. The choice of p depends on the overall probability of error of the QSA. Below we show that, by choosing $|o_{\pm j, m=0}| = \mathcal{O}(\nu)$, with $\nu = \Delta\beta E_M$, the QSA is guaranteed to succeed with a probability of error of order $\mathcal{O}(\epsilon)$. Furthermore, since $\min_{j, \beta} \{\varphi_j(\beta)\} = \mathcal{O}(\sqrt{\delta})$, where δ is the minimum spectral gap of $M(\beta)$, it is enough to choose p such that $2^p = \mathcal{O}(1/(\nu\sqrt{\delta}))$, giving a implementation complexity for each phase estimation $\mathcal{N}_{PEA} = \mathcal{O}(1/(\nu\sqrt{\delta}))$.

To obtain the implementation complexity of the QSA, it is helpful to consider the equivalent case where non of the measurements are actually performed until after the final PEA [22]. The input state to the first PEA is $|0_1 \psi_0(0)\rangle$, where we introduce the subscripts $1, \dots, q$ to denote the sets of p qubits used as ancillae in each PEA. The first PEA is performed at inverse temperature β_1 . From Eq. (17)

$$|0_1 \psi_0(0)\rangle = (1 - \mathcal{O}(\nu^2)) |0_1 \psi_0(\beta_1)\rangle + \mathcal{O}(\nu) |0_1 \psi_0^\perp(\beta_1)\rangle. \quad (\text{B6})$$

Also [Eq. (16)],

$$|\psi_0^\perp(\beta_1)\rangle = \sum_{j=1}^{d-1} \frac{e_j}{\sqrt{2}} [|\psi_{+j}(\beta_1)\rangle + |\psi_{-j}(\beta_1)\rangle]. \quad (\text{B7})$$

After the implementation of the unitary $PE(\beta_1)$ (see Fig. 2), the evolved state is

$$\begin{aligned} &(1 - \mathcal{O}(\nu^2)) |0_1 \psi_0(\beta_1)\rangle \\ &+ \mathcal{O}(\nu) \sum_{j, m} \frac{e_j}{\sqrt{2}} [o_{+j, m} |m_1 \psi_{+j}(\beta_1)\rangle + o_{-j, m} |m_1 \psi_{-j}(\beta_1)\rangle]. \end{aligned} \quad (\text{B8})$$

Since only the states with $m_1 = 0$ in the above sum contribute to the final probability of projecting onto $|0_1\rangle$ at the end of the

first PEA, it is convenient to rewrite Eq. (B8) as

$$(1 - \mathcal{O}(\nu^2)) |0_1 \psi_0(\beta_1)\rangle + \mathcal{O}(\nu^2) |0_1 \psi_0^\perp(\beta_1)\rangle + \mathcal{O}(\nu) |\chi_1\rangle. \quad (\text{B9})$$

Here, $\langle \psi_0(\beta_1) | \psi_0^\perp(\beta_1) \rangle = \langle 0_1 | \chi_1 \rangle = 0$ and the order of the second term follows from the previous choice of p so that $|o_{\pm j, m=0}| = \mathcal{O}(\nu)$.

We now introduce the state $|0_2\rangle$ for the second set of p qubits, and evolve with the action of $PE(\beta_2)$. The output of the second phase estimation gives [Eq. (17)]

$$\begin{aligned} &(1 - \mathcal{O}(\nu^2)) |0_2 0_1 \psi_0(\beta_1)\rangle + \mathcal{O}(\nu^2) |0_2 0_1 \psi_0^\perp(\beta_2)\rangle \\ &+ \mathcal{O}(\nu^2) PE(\beta_2) |0_2 0_1 \psi_0^\perp(\beta_1)\rangle + \mathcal{O}(\nu) |\chi_2\rangle, \end{aligned} \quad (\text{B10})$$

with $\langle 0_1 0_2 | \chi_2 \rangle = 0$.

We repeat this procedure by introducing the states $|0_3\rangle, \dots, |0_q\rangle$ and by evolving with $PE(\beta_3), \dots, PE(\beta_Q = \beta_f)$, respectively. Denote by $|\xi\rangle$ the evolved (joint) state of all the registers $1, \dots, q$ and $\mathcal{H}_A \otimes \mathcal{H}_B$. After the measurement on $1, \dots, q$, the probability of projecting onto $|0_q \dots 0_1\rangle$ is given by $\mathcal{P}_0 = \langle \xi | P_0 | \xi \rangle$, with $P_0 = |0_q \dots 0_1\rangle \langle 0_q \dots 0_1|$ the projector onto the corresponding subspace. By a similar analysis as the ones performed above for the first two steps, we obtain

$$\begin{aligned} P_0 |\xi\rangle &\equiv (1 - \mathcal{O}(\nu^2))^Q |0_q \dots 0_1 \psi_0(\beta_f)\rangle + \\ &\mathcal{O}(\nu^2) P_0 \sum_{i=0}^{Q-1} PE(\beta_Q) \dots PE(\beta_{Q-i+1}) |0_q \dots 0_1 \psi_0^\perp(\beta_{Q-i})\rangle. \end{aligned} \quad (\text{B11})$$

Thus the probability of $\mathcal{H}_A \otimes \mathcal{H}_B$ being in the desired state $|\psi_0(\beta_f)\rangle$ can be bounded below, by using Eq. (B11), as

$$\begin{aligned} \mathcal{P}_0 &\geq \left[(1 - \mathcal{O}(\nu^2))^Q - (Q-1) \mathcal{O}(\nu^2) \right]^2 \\ &\geq 1 - \tau' Q \nu^2, \end{aligned} \quad (\text{B12})$$

for some constant $\tau' = \mathcal{O}(1)$.

Assume now that the state of $\mathcal{H}_A \otimes \mathcal{H}_B$ is $|\psi_0(\beta_f)\rangle = |\phi_0(\beta_f) \circ\rangle = \sum_{\sigma=1}^d \sqrt{\pi^\sigma(\beta_f)} |\sigma \circ\rangle$. If a measurement on the $|\sigma\rangle$ -basis is performed on \mathcal{H}_A , the probability of finding the system in an excited state can be bounded by $d e^{-\beta_f \gamma}$, with γ the spectral gap of E . Thus, after the QSA, the total probability of such an event, which is the error probability for QSA, can be bounded above by

$$\mathcal{P}(\sigma \notin \mathbb{S}_0) \leq d e^{-\beta_f \gamma} + \tau' Q \nu^2, \quad (\text{B13})$$

as claimed.

[1] W.J. Cook, W.H. Cunningham, W.R. Pulleyblank, and A. Schrijver, *Combinatorial Optimization*, J. Wiley and Sons, New York (1998).

[2] S. Kirkpatrick, C.D. Gelett, and M.P. Vecchi, *Science* **220**, 671 (1983).

[3] M.E.J. Newman and G.T. Barkema, *Monte Carlo Methods*

- in *Statistical Physics*, Oxford University Press, Oxford, UK (1999).
- [4] D.W. Stroock, *An Introduction to Markov Processes*, Springer-Verlag, Berlin (2005).
 - [5] F. Barahona, J. Phys. A **15**, 3241 (1982).
 - [6] T. Kadowaki and H. Nishimori, Phys. Rev. E **58**, 5355 (1998); G.E. Santoro *et al.*, Science **295**, 2427 (2002); G.E. Santoro and E. Tosatti, Nature Physics **3**, 593 (2007).
 - [7] R.D. Somma, C.D. Batista, and G. Ortiz, Phys. Rev. Lett. **99**, 030603 (2007).
 - [8] E. Farhi, *et al.*, Science **292**, 472 (2001).
 - [9] P. Shor, *Proceedings of the 35th Annual Symp. Found. Comp. Science*, 116 (1994); L.K. Grover, *Proceedings of the 28th Annual ACM Symp. on the Th. Comp.*, 212 (1996).
 - [10] M. Szegedy, *Proceedings of the 45th IEEE Symposium on Foundations of Computer Science*, 32 (2004).
 - [11] A. Ambainis, *Proceedings of the 45th Symposium on Foundations of Computer Science*, 22 (2004).
 - [12] R. Cleve, A. Ekert, C. Macchiavello, and M. Mosca, Proc. R. Soc. Lon. A **454**, 339 (1998).
 - [13] M. Nielsen and I. Chuang, *Quantum Computation and Quantum Information*, Cambridge University Press, Cambridge, UK (2000).
 - [14] B. Misra and E.C.G. Sudarshan, J. Math. Phys. **18**, 756 (1977).
 - [15] W.M. Itano, D.J. Heinzen, J.J. Bollinger, and D.J. Wineland, Phys. Rev. A **41**, 2295 (1990).
 - [16] S. Geman and D. Geman, IEEE Trans. Pattern. Anal. Mach. Intell. **6**, 721 (1984).
 - [17] F. Magniez, A. Nayak, J. Roland, and M. Santha, *Proceedings of the 39th Annual ACM Symposium on Theory of Computing*, 575 (2007).
 - [18] D.J. Aldous, J. London Math. Soc. (2) **25**, 564 (1981).
 - [19] A. Ambainis, *et al.*, *Proceedings of the 33th Annual ACM Symposium on Theory of Computing*, 37 (2001).
 - [20] See J. Kempe, arXiv:quant-ph/0303081 for a review and references therein.
 - [21] E. Knill, G. Ortiz, R. Somma, Phys. Rev. A **75**, 012328 (2007).
 - [22] A.M. Childs, *et al.*, Phys. Rev. A **66**, 032314 (2002).
 - [23] P.C. Richter, Phys. Rev. A **76**, 042306 (2007).
 - [24] A. Messiah, *Quantum Mechanics*, Dover Publications, New York (1999).
 - [25] Note that the rate $\Delta\beta$ can be chosen to be β -dependent if the gap of $M(\beta)$ is used on the right side of Eq. (A7) instead of δ . However, the overall implementation complexity of SA will still be dominated by the minimum gap.
 - [26] R. Somma, G. Ortiz, J.E. Gubernatis, E. Knill, and R. Laflamme, Phys. Rev. A **65**, 042323/1 (2002).